Journal of Operation and Automation in Power Engineering
Vol. 8, No. 2, Aug. 2020, Pages: 128-140
http://joape.uma.ac.ir

A Model-Based PDPC Method for Control of BDFRG under Unbalanced Grid Voltage Condition Using Power Compensation Strategy

M. Moazen[1], R. Kazemzadeh[2,], M. R. Azizian[2]*

[1]*Department of Electrical Engineering, University of Bonab, Bonab, Iran.*
[2]*Department of Electrical Power Engineering, Sahand University of Technology, Tabriz, Iran.*

Abstract- *Brushless doubly fed reluctance generator (BDFRG) has been recently suggested as a wind generator. Different control methods are presented in literature for the BDFRG, but there is a gap on control under unbalanced grid voltage condition (UGVC). This paper presents a predictive direct power control (PDPC) method for the BDFRG under UGVC. The proposed PDPC method is based on power compensation strategy, and aims to balance the BDFRG current (strategy I), and to remove the electrical torque pulsation (strategy II). The control objectives are defined using the BDFRG positive sequence (PS) and negative sequence (NS) equations. Then, the active power and reactive power variations are predicted to compute the required voltage for the BDFRG control winding. Finally, the BDFRG is controlled by applying the calculated voltage to the control winding. Simulink toolbox of MATLAB software is used to simulate the system model. Both the proposed PDPC method (with strategies I & II) and the original PDPC method (without a compensation strategy) are applied to control of the BDFRG under UGVC, and the results are compared. The results show the good performance of the proposed PDPC method.*

Keyword: Brushless doubly fed reluctance generator, power compensation strategy, predictive direct power control, unbalanced grid voltage, wind power.

1. INTRODUCTION

Nowadays, the brushless doubly fed reluctance generator (BDFRG) has been offered for wind power systems as a suitable choice [1, 2], because of the comparable performance of the BDFRG with doubly fed induction generator (DFIG) [3, 4] and brushless doubly fed induction generator (BDFIG) [5]. Similar to the DFIG and BDFIG in wind power applications, the BDFRG utilizes fractional converter [6, 7]. The main advantages of the BDFRG are its reasonable cost and high reliability because of the brushless structure [5, 7]. Absence of brushes and slip rings in the BDFRG decreases the maintenance cost and increases the reliability (against the DFIG), which both are important especially in off-shore plants [8, 9]. In comparison with the BDFIG, the BDFRG is more efficient [10], and its control is easier [7] because of the cageless rotor.

Stator of the BDFRG has two sets of three-phase windings, which are called primary (or power) winding and secondary (or control) winding. The primary and secondary windings have different pole pairs, and are supplied with different frequencies. The coupling between them is made by a reluctance rotor, where the number of its salient poles, P_r, is equal to the total number of the primary and secondary pole pairs, P_1 and P_2. The primary winding is directly connected to the grid, and the secondary winding is connected by a bi-directional back to back converter [6]. Each converter consists of 6 IGBT/Diode switches to convert three-phase AC power to DC power, and vice versa. The two converters have a common DC link. Connection of the BDFRG to the grid and wind turbine has been shown in Fig. 1 [11].

Different control methods, which have been presented for the BDFRG in literature, can be categorized as follows: Scalar control [12-15] is the simplest method with slow dynamic response. Vector control [16-18] and field orientation control [19, 20], which are two similar methods respectively based on voltage and flux orientation, can be located in the category of vector methods. Dynamic response of the vector methods is faster than scalar control methods. Also, switching frequency of the vector methods is constant. However, precise tuning of PI controllers is required. The third category is dedicated to direct meth-

Received: 01 Oct. 2018
Revised: 07 Jun. 2019 and 19 Jul. 2019
Accepted: 26 Aug. 2019
∗Corresponding author:
E-mail: r.kazemzadeh@sut.ac.ir (R. Kazemzadeh)
Digital object identifier: 10.22098/joape.2020.5286.1392
Research paper

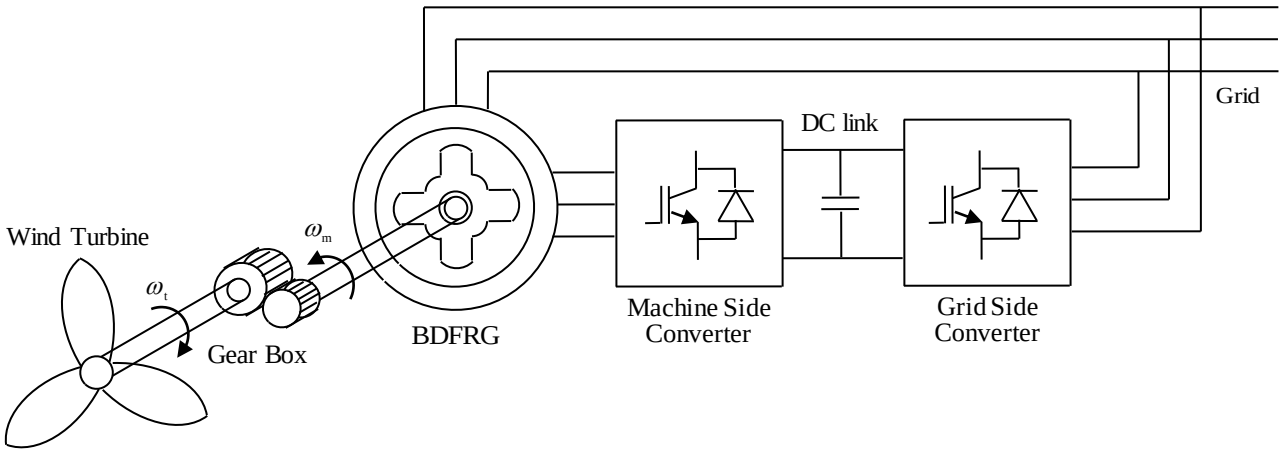

Fig. 1. Connection of the BDFRG to the grid and wind turbine [11]

-ods such as: direct torque control [21], torque and reactive power control [22], direct power control [8], and hysteresis control [23]. The main advantages of the direct methods are the fast dynamic response, and no need to PI controllers. However, variable switching frequency is their disadvantage. Predictive direct power control (PDPC) [24] is a model based method, which simultaneously has the advantages such as: fast dynamic response, fixed switching frequency, and no need to PI controllers. However, parameter determination is required in model based control methods. Parameter determination of the BDFRG has been presented in Ref. [25]. Model based methods can also be used to sensorless speed control. References [26-28] propose model reference adaptive system control to sensorless speed control of the BDFRG.

To the authors' knowledge, all of the above control methods are related to balanced condition, and control of the BDFRG under unbalanced grid voltage condition (UGVC) has not been studied up to now. By locating wind power plants in remote areas, they usually experience UGVC [29, 30]. The unbalanced voltage of the grid causes some problems in the BDFRG operation such as unbalanced current of the primary, harmonics in the secondary current, power and torque pulsations [31], and consequently, localized temperature increase in the stator and additional stress on the mechanical parts [29, 30]. These problems may force wind generator to be disconnected from the grid [32], and consequently the stability of the grid can be weakened [33]. The proper control of the wind generator under UGVC can resolve these problems.

To study the UGVC operation of the BDFRG, and to have a proper control method, positive sequence (PS) and negative sequence (NS) equations of the BDFRG should be determined. These equations were previously developed in Ref. [31], and the BDFRG operation (without any controller) was analysed. On the other hand, PDPC method was presented for control of the BDFRG under balanced condition in Ref. [24]. The PDPC method directly controls active power and reactive power, and has fixed switching frequency and fast dynamic response, simultaneously. In the current paper, the BDFRG is controlled under UGVC by a new proposed PDPC method. The PS and NS equations of the BDFRG are used to develop the proposed PDPC method. The proposed PDPC method is based on power compensation strategy [34, 35], and aims to achieve the following control objectives: (1) balancing of the primary current (strategy I), and (2) elimination of the electrical torque pulsation (strategy II). The next sections have been managed as follows: space vector model of the BDFRG has been expressed in Section 2. In Section 3, the original PDPC method for control of the BDFRG has been introduced, briefly. In Section 4, UGVC equations of the BDFRG in PS and NS have been presented. The proposed PDPC method (strategies I & II) has been presented in Section 5 for control of the BDFRG under UGVC. In Section 6, UGVC operation of the BDFRG with both the original PDPC method and the proposed PDPC method (strategies I & II) has been studied and compared. Finally, Section 7 has been dedicated to conclusion.

2. SPACE VECTOR MODEL OF THE BDFRG

Space vector model of the BDFRG, in a rotating reference frame at ω, is as follows [36, 37]:

$$\boldsymbol{v}_p = R_p \boldsymbol{i}_p + \frac{d\boldsymbol{\lambda}_p}{dt} + j\omega\boldsymbol{\lambda}_p \tag{1}$$

$$\boldsymbol{v}_s = R_s \boldsymbol{i}_s + \frac{d\boldsymbol{\lambda}_s}{dt} + j(\omega_r - \omega)\boldsymbol{\lambda}_s \tag{2}$$

$$\boldsymbol{\lambda_p} = L_p \boldsymbol{i_p} + L_{ps} \boldsymbol{i_s^*} \tag{3}$$

$$\boldsymbol{\lambda_s} = L_s \boldsymbol{i_s} + L_{ps} \boldsymbol{i_p^*} \tag{4}$$

Where, R_p is resistance of the primary, R_s is resistance of the secondary, L_p is inductance of the primary, L_s is inductance of the secondary, and L_{ps} is mutual inductance of the primary to the secondary. Also, $\boldsymbol{x_p}$ is a space vector of the primary variables, $\boldsymbol{x_s}$ is a space vector of the secondary variables, and ω_r is the electrical angular velocity of the rotor [6]:

$$\omega_r = \omega_p + \omega_s \tag{5}$$

Where, ω_p and ω_s are the angular frequencies of the primary and secondary, respectively. The primary equations are stated in a frame rotating at ω, and the secondary equations are stated in a frame rotating at ω_r - ω [36]. The BDFRG electrical torque expression is as follows [37]:

$$T_e = j(3/4)P_r \left\{ \boldsymbol{\lambda_p} \boldsymbol{i_p^*} - \boldsymbol{\lambda_p^*} \boldsymbol{i_p} \right\} \tag{6}$$

3. PDPC FOR THE BDFRG

PDPC for the BDFRG [24] consists of two following steps:

- Computation of the required voltage of the secondary, based on prediction of primary power variation in a specific sampling time interval (T_s), to remove power error at the end of T_s.
- Selection of proper voltage vectors in T_s by space vector pulse width modulation (SVPWM) method, to achieve the calculated voltage for the secondary winding.

The required voltage of the secondary is calculated by PDPC method over k^{th} T_s in rotor reference frame, as follows [24]:

$$v_{sd}(k) = -\omega_r(k)\lambda_{sq}(k) - \left(2\sigma L_s \Delta Q_p(k) / 3T_s \omega_p \lambda_{psd}(k)\right) \tag{7}$$

$$v_{sq}(k) = \omega_r(k)\lambda_{sd}(k) + \left(2\sigma L_s \Delta P_p(k) / 3T_s \omega_p \lambda_{psd}(k)\right) \tag{8}$$

Where, $\sigma = 1 - L_{ps}^2 / L_p L_s$ and $\lambda_{psd} = \left(L_{ps} / L_p\right)\lambda_p$ [24]. Also, $\Delta P_p(k)$ and $\Delta Q_p(k)$ are the required active power and reactive power variations over k^{th} T_s:

$$\Delta P_p(k) = P_p^*(k) - P_p(k) \tag{9}$$

$$\Delta Q_p(k) = Q_p^*(k) - Q_p(k) \tag{10}$$

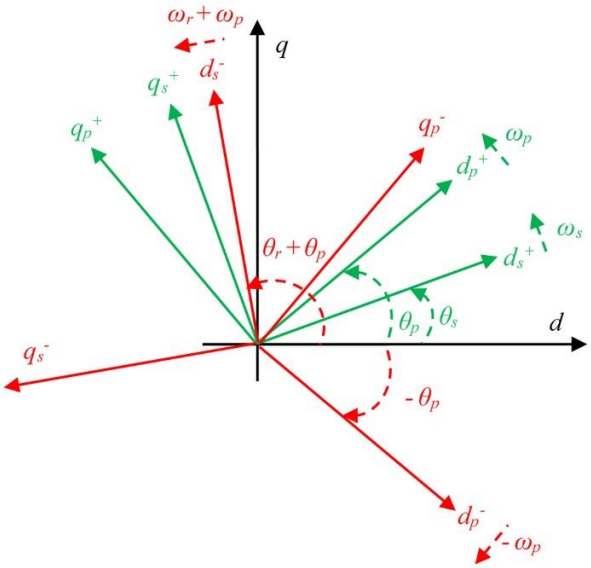

Fig. 2. The BDFRG reference frames under UGVC [31]

Where, $P_p(k)$, $P_p^*(k)$, $Q_p(k)$, and $Q_p^*(k)$ are respectively the primary active power, its reference value, the primary reactive power, and its reference value over k^{th} T_s. The machine side converter uses SVPWM [38] to generate the calculated voltage for the secondary.

4. THE BDFRG EQUATIONS UNDER UGVC

Fig. 2 illustrates the BDFRG reference frames under UGVC. The stationary reference frame is shown with dq. Angular speed and angle of rotating reference frames are stated respect to dq frame. The primary reference frame for positive sequence is dq_p^+, which is rotating at ω_p and with angle of θ_p. The secondary reference frame for positive sequence is dq_s^+, which is rotating at ω_s and with angle of θ_s. The primary reference frame for negative sequence is dq_p^-, which is rotating at $-\omega_p$ and with angle of $-\theta_p$. The secondary reference frame for positive sequence is dq_s^-, which is rotating at $\omega_p + \omega_r$ and with angle of $\theta_p + \theta_r$.

When the zero sequence component is ignored, the PS equations of the BDFRG primary (in dq_p^+ frame) and secondary (in dq_s^+ frame) are as follows [31]:

$$v_{pd}^+ = R_p i_{pd}^+ + \frac{d\lambda_{pd}^+}{dt} - \omega_p \lambda_{pq}^+ \tag{11}$$

$$v_{pq}^+ = R_p i_{pq}^+ + \frac{d\lambda_{pq}^+}{dt} + \omega_p \lambda_{pd}^+ \tag{12}$$

$$v_{sd}^+ = R_s i_{sd}^+ + \frac{d\lambda_{sd}^+}{dt} - \omega_s \lambda_{sq}^+ \tag{13}$$

$$v_{sq}^{+} = R_s i_{sq}^{+} + \frac{d\lambda_{sq}^{+}}{dt} + \omega_s \lambda_{sd}^{+} \tag{14}$$

Correspondingly, the NS equations of the BDFRG primary (in dq_p^- frame) and secondary (in dq_s^- frame) are as follows [31]:

$$v_{pd}^{-} = R_p i_{pd}^{-} + \frac{d\lambda_{pd}^{-}}{dt} + \omega_p \lambda_{pq}^{-} \tag{15}$$

$$v_{pq}^{-} = R_p i_{pq}^{-} + \frac{d\lambda_{pq}^{-}}{dt} - \omega_p \lambda_{pd}^{-} \tag{16}$$

$$v_{sd}^{-} = R_s i_{sd}^{-} + \frac{d\lambda_{sd}^{-}}{dt} - (\omega_r + \omega_p)\lambda_{sq}^{-} \tag{17}$$

$$v_{sq}^{-} = R_s i_{sq}^{-} + \frac{d\lambda_{sq}^{-}}{dt} + (\omega_r + \omega_p)\lambda_{sd}^{-} \tag{18}$$

Based on the above equations, the BDFRG primary powers can be obtained as follows [31]:

$$\begin{aligned} P_p = 1.5\{&\left(v_{pd}^{+} i_{pd}^{+} + v_{pq}^{+} i_{pq}^{+} + v_{pd}^{-} i_{pd}^{-} + v_{pq}^{-} i_{pq}^{-}\right) \\ &+ \left(v_{pd}^{+} i_{pd}^{-} + v_{pq}^{+} i_{pq}^{-} + v_{pd}^{-} i_{pd}^{+} + v_{pq}^{-} i_{pq}^{+}\right)\cos(2\omega_p t) \\ &+ \left(v_{pd}^{+} i_{pq}^{-} - v_{pq}^{+} i_{pd}^{-} - v_{pd}^{-} i_{pq}^{+} + v_{pq}^{-} i_{pd}^{+}\right)\sin(2\omega_p t)\} \end{aligned} \tag{19}$$

$$\begin{aligned} Q_p = 1.5\{&\left(-v_{pd}^{+} i_{pq}^{+} + v_{pq}^{+} i_{pd}^{+} - v_{pd}^{-} i_{pq}^{-} + v_{pq}^{-} i_{pd}^{-}\right) \\ &+ \left(-v_{pd}^{+} i_{pq}^{-} + v_{pq}^{+} i_{pd}^{-} - v_{pd}^{-} i_{pq}^{+} + v_{pq}^{-} i_{pd}^{+}\right)\cos(2\omega_p t) \\ &+ \left(v_{pd}^{+} i_{pd}^{-} + v_{pq}^{+} i_{pq}^{-} - v_{pd}^{-} i_{pd}^{+} - v_{pq}^{-} i_{pq}^{+}\right)\sin(2\omega_p t)\} \end{aligned} \tag{20}$$

Also, the BDFRG electrical torque expression under UGVC is as follows [31]:

$$\begin{aligned} T_e = 1.5P_r\{&\left(\lambda_{pd}^{+} i_{pq}^{+} - \lambda_{pq}^{+} i_{pd}^{+} + \lambda_{pd}^{-} i_{pq}^{-} - \lambda_{pq}^{-} i_{pd}^{-}\right) \\ &+ \left(\lambda_{pd}^{+} i_{pq}^{-} - \lambda_{pq}^{+} i_{pd}^{-} + \lambda_{pd}^{-} i_{pq}^{+} - \lambda_{pq}^{-} i_{pd}^{+}\right)\cos(2\omega_p t) \\ &+ \left(-\lambda_{pd}^{+} i_{pd}^{-} - \lambda_{pq}^{+} i_{pq}^{-} + \lambda_{pd}^{-} i_{pd}^{+} + \lambda_{pq}^{-} i_{pq}^{+}\right)\sin(2\omega_p t)\} \end{aligned} \tag{21}$$

The primary powers and electrical torque expressions are consist of two oscillating parts at $2\omega_p$. Therefore, the BDFRG electrical torque and powers are pulsating under UGVC when there is not any control.

5. PDPC FOR THE BDFRG UNDER UGVC

In this section, the PDPC method has been developed for control of the BDFRG under UGVC by using the power compensation strategy. In steady state and by ignoring copper losses, the PS and NS components of the primary flux in the respective *dq* frames can be obtained from Eqns. (11), (12), (15) and (16) as follows:

$$\lambda_{pq}^{+} = -v_{pd}^{+} / \omega_p \tag{22}$$

$$\lambda_{pd}^{+} = v_{pq}^{+} / \omega_p \tag{23}$$

$$\lambda_{pq}^{-} = v_{pd}^{-} / \omega_p \tag{24}$$

$$\lambda_{pd}^{-} = -v_{pq}^{-} / \omega_p \tag{25}$$

By substituting Eqns. (22) - (25) into Eq. (21), the electrical torque can be expressed by the PS and NS components of the primary voltages and currents as:

$$\begin{aligned} T_e = \left(1.5P_r/\omega_p\right)\{&\left(v_{pd}^{+} i_{pd}^{+} + v_{pq}^{+} i_{pq}^{+} - v_{pd}^{-} i_{pd}^{-} - v_{pq}^{-} i_{pq}^{-}\right) \\ &+ \left(v_{pd}^{+} i_{pd}^{-} + v_{pq}^{+} i_{pq}^{-} - v_{pd}^{-} i_{pd}^{+} - v_{pq}^{-} i_{pq}^{+}\right)\cos(2\omega_p t) \\ &+ \left(v_{pd}^{+} i_{pq}^{-} - v_{pq}^{+} i_{pd}^{-} + v_{pd}^{-} i_{pq}^{+} - v_{pq}^{-} i_{pd}^{+}\right)\sin(2\omega_p t)\} \end{aligned} \tag{26}$$

Now, A_1, A_2, B_1 and B_2 are defined as follows:

$$A_1 = v_{pd}^{+} i_{pd}^{-} + v_{pq}^{+} i_{pq}^{-} \tag{27}$$

$$A_2 = v_{pd}^{+} i_{pq}^{-} - v_{pq}^{+} i_{pd}^{-} \tag{28}$$

$$B_1 = v_{pd}^{-} i_{pd}^{+} + v_{pq}^{-} i_{pq}^{+} \tag{29}$$

$$B_2 = -v_{pd}^{-} i_{pq}^{+} + v_{pq}^{-} i_{pd}^{+} \tag{30}$$

Therefore, the primary power equations (i.e. (19) and (20)) and the electrical torque equation (i.e. (26)) can be rewritten as:

$$\begin{aligned} P_p = &P_{p\_av} \\ &+ 1.5\left(\left(A_1 + B_1\right)\cos(2\omega_p t) + \left(A_2 + B_2\right)\sin(2\omega_p t)\right) \end{aligned} \tag{31}$$

$$\begin{aligned} Q_p = &Q_{p\_av} \\ &+ 1.5\left(\left(-A_2 + B_2\right)\cos(2\omega_p t) + \left(A_1 - B_1\right)\sin(2\omega_p t)\right) \end{aligned} \tag{32}$$

$$\begin{aligned} T_e = &T_{e\_av} + \left(1.5P_r/\omega_p\right) \\ &\cdot\left(\left(A_1 - B_1\right)\cos(2\omega_p t) + \left(A_2 - B_2\right)\sin(2\omega_p t)\right) \end{aligned} \tag{33}$$

Where, P_{p_av}, Q_{p_av} and T_{e_av} are non-oscillating parts of the primary active power, primary reactive power, and the electrical torque, respectively, as:

$$P_{p\_av} = 1.5\left(v_{pd}^{+} i_{pd}^{+} + v_{pq}^{+} i_{pq}^{+} + v_{pd}^{-} i_{pd}^{-} + v_{pq}^{-} i_{pq}^{-}\right) \tag{34}$$

$$Q_{p\_av} = 1.5\left(-v_{pd}^{+} i_{pq}^{+} + v_{pq}^{+} i_{pd}^{+} - v_{pd}^{-} i_{pq}^{-} + v_{pq}^{-} i_{pq}^{-}\right) \tag{35}$$

$$T_{e\_av} = \left(1.5P_r/\omega_p\right)\left(v_{pd}^{+} i_{pd}^{+} + v_{pq}^{+} i_{pq}^{+} - v_{pd}^{-} i_{pd}^{-} - v_{pq}^{-} i_{pq}^{-}\right) \tag{36}$$

Equations (31) - (33) are used in the power compensation strategy of the proposed PDPC method to control the BDFRG under UGVC. Two main objectives can be defined for the power compensation strategy: (1) to balance the primary current, and (2) to eliminate the electrical torque pulsation.

5.1. Strategy I

Unbalanced current of the primary leads to localized temperature increase in the stator. Therefore, having a balanced primary current is important to have a uniform heat distribution in the BDFRG stator. To achieve balanced current in the BDFRG primary (control objective), it is required to remove the NS component of the primary current. According to equations (27) and (28), if A_1 and A_2 are simultaneously controlled to be zero, the NS component of the primary current will be removed. In the other words, for rejection of the NS component of the primary current, A_1 and A_2 expressions must be kept zero:

$$A_1 = v_{pd}^{+} i_{pd}^{-} + v_{pq}^{+} i_{pq}^{-} = 0 \tag{37}$$

$$A_2 = v_{pd}^{+} i_{pq}^{-} - v_{pq}^{+} i_{pd}^{-} = 0 \tag{38}$$

$P_{p\_unb}^{*}$ and $Q_{p\_unb}^{*}$ are defined as new active power and reactive power references, which result in balanced primary current:

$$P_{p\_unb}^{*} = P_{p\_b}^{*} + P_{p\_comp}^{*} \tag{39}$$

$$Q_{p\_unb}^{*} = Q_{p\_b}^{*} + Q_{p\_comp}^{*} \tag{40}$$

Where, $P_{p\_b}^{*}$, $P_{p\_comp}^{*}$, $Q_{p\_b}^{*}$, and $Q_{p\_comp}^{*}$ are the original active power reference under balanced condition, the compensating active power reference under UGVC, the original reactive power reference under balanced condition, and the compensating reactive power reference under UGVC, respectively. Equations (39) and (40) can be rewritten as:

$$P_{p\_b}^{*} = P_{p\_unb}^{*} - P_{p\_comp}^{*} \tag{41}$$

$$Q_{p\_b}^{*} = Q_{p\_unb}^{*} - Q_{p\_comp}^{*} \tag{42}$$

The primary active power and reactive power will be controlled to achieve $P_{p\_unb}^{*}$ and $Q_{p\_unb}^{*}$, respectively. So, $P_{p\_unb}^{*}$ and $Q_{p\_unb}^{*}$ in Eqns. (41) - (42) can be substituted by Eqns. (31) - (32). When Eqns. (37) - (38) are satisfied, Eqns. (41) - (42) can be rewritten as:

$$P_{p\_b}^{*} = P_{p\_av} + 1.5\left(B_1 \cos(2\omega_p t) + B_2 \sin(2\omega_p t)\right) - P_{p\_comp}^{*} \tag{43}$$

$$Q_{p\_b}^{*} = Q_{p\_av} + 1.5\left(B_2 \cos(2\omega_p t) - B_1 \sin(2\omega_p t)\right) - Q_{p\_comp}^{*} \tag{44}$$

The left hand side of Eqns. (43) and (44) is constant, so the right hand side of both equations, which contains both constant and oscillating parts, must be constant, too. $P_{p\_comp}^{*}$ and $Q_{p\_comp}^{*}$, which make the right hand side of Eqns. (43) and (44) constant, are as follows:

$$P_{p\_comp}^{*} = 1.5\left(B_1 \cos(2\omega_p t) + B_2 \sin(2\omega_p t)\right) \tag{45}$$

$$Q_{p\_comp}^{*} = 1.5\left(B_2 \cos(2\omega_p t) - B_1 \sin(2\omega_p t)\right) \tag{46}$$

The new power references can be achieved by substituting Eqns. (45) and (46) into Eqns. (39) and (40), respectively, as:

$$P_{p\_unb}^{*} = P_{p\_b}^{*} + 1.5\left(B_1 \cos(2\omega_p t) + B_2 \sin(2\omega_p t)\right) \tag{47}$$

$$Q_{p\_unb}^{*} = Q_{p\_b}^{*} + 1.5\left(B_2 \cos(2\omega_p t) - B_1 \sin(2\omega_p t)\right) \tag{48}$$

These new power references will force A_1 and A_2 to be zero. Therefore, the NS component of the primary current will be removed, and the balanced primary current will be achieved.

5.2. Strategy II

Another control objective under UGVC is defined as cancelation of the electrical torque pulsation. Electrical torque pulsation leads to additional stress on mechanical parts. Therefore, removing electrical torque pulsation is important to reduce extra stress on the mechanical parts. According to Eq. (33), the oscillating parts of the electrical torque will be eliminated, if A_1 and A_2 are equal with B_1 and B_2, respectively:

$$A_1 = B_1 \tag{49}$$

$$A_2 = B_2 \tag{50}$$

Again, $P_{p\_unb}^{*}$ and $Q_{p\_unb}^{*}$ are defined as new active power and reactive power references, which result in elimination of the electrical torque pulsation:

$$P_{p\_unb}^{*} = P_{p\_b}^{*} + P_{p\_comp}^{*} \tag{51}$$

$$Q_{p\_unb}^{*} = Q_{p\_b}^{*} + Q_{p\_comp}^{*} \tag{52}$$

Where, $P_{p\_comp}^{*}$ and $Q_{p\_comp}^{*}$ are the compensating active power and reactive power references under UGVC for elimination of the electrical torque pulsation, respectively. Equations (51) and (52) can be rewritten as:

$$P_{p\_b}^{*} = P_{p\_unb}^{*} - P_{p\_comp}^{*} \tag{53}$$

$$Q_{p\_b}^{*} = Q_{p\_unb}^{*} - Q_{p\_comp}^{*} \tag{54}$$

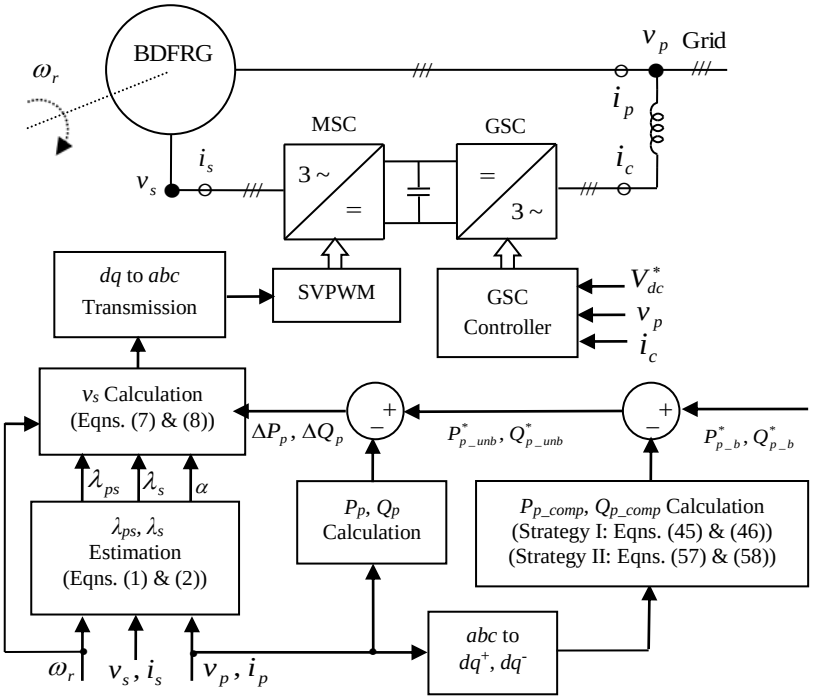

Fig. 3. Block diagram of the proposed PDPC method under UGVC

$P_{p\_unb}^*$ and $Q_{p\_unb}^*$ in Eqns. (53)-(54) can be substituted by Eqns. (31) - (32). When Eqns. (49) and (50) are satisfied, Eqns. (53) and (54) can be rewritten as:

$$P_{p\_b}^* = P_{p\_av} + 3\left(B_1\cos(2\omega_p t) + B_2\sin(2\omega_p t)\right) - P_{p\_comp}^* \quad (55)$$

$$Q_{p\_b}^* = Q_{p\_av} - Q_{p\_comp}^* \quad (56)$$

To make the right hand side of Eqns. (55) and (56) constant, $P_{p\_comp}^*$ and $Q_{p\_comp}^*$ must be chosen as:

$$P_{p\_comp}^* = 3\left(B_1\cos(2\omega_p t) + B_2\sin(2\omega_p t)\right) \quad (57)$$

$$Q_{p\_comp}^* = 0 \quad (58)$$

The new power references are obtained by substituting Eqns. (57) and (58) into Eqs. (51) and (52), respectively:

$$P_{p\_unb}^* = P_{p\_b}^* + 3\left(B_1\cos(2\omega_p t) + B_2\sin(2\omega_p t)\right) \quad (59)$$

$$Q_{p\_unb}^* = Q_{p\_b}^* \quad (60)$$

Therefore, only by adding $P_{p\_comp}^*$ (i.e. (57)) to the original active power reference, A_1 and A_2 will be forced to be B_1 and B_2, respectively. So, the electrical torque pulsation will be eliminated. Block diagram of the proposed PDPC method under UGVC is shown in Fig. 3.

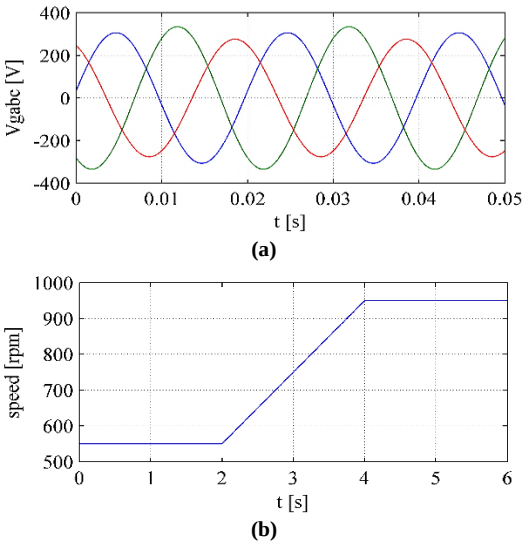

Fig. 4. (a) The three-phase unbalanced voltage of the grid, (b) the BDFRG speed curve

6. SIMULATION RESULTS AND DISCUSSION

To study the operation of the BDFRG under UGVC and the performance of the proposed PDPC method, the BDFRG model has been simulated in MATLAB/Simulink software. The BDFRG parameters can be found in Ref. [39]. In the next three subsections, the operation of the BDFRG has been tested under UGVC by the original PDPC method, strategy I, and strategy II of the proposed PDPC method. The tests are performed under unbalanced grid voltage which is illustrated in Fig. 4(a). The grid voltage contains PS component with 373.5 V, 50 Hz, and NS component with 41.5 V, 50 Hz (unbalance factor = 11.11%). The

speed curve, which is shown in Fig. 4(b), covers all the BDFRG operating modes, i.e. sub-synchronous, synchronous, and super-synchronous speeds. In addition, a test for better comparison of the control methods has been designed, and the simulation results have been reported in the fourth subsection. Furthermore, the performance of the control methods under different unbalanced voltage dips has been studied in the fifth subsection. It should be mentioned that all results are related to post-startup period. Also, the grid side converter is controlled by a PDPC method for control of rectifier [40].

6.1. Control of the BDFRG under UGVC using original PDPC method

In this subsection, the BDFRG operation under UGVC has been studied by applying the original PDPC method. The primary active power and reactive power references are -1000 W and 0 Var, respectively. In Fig. 5, the primary powers and their references are illustrated, where a good power tracking can be observed. In addition, the power pulsation is not considerable under UGVC due to the precise control of the primary powers. The negative sign of the power indicates generation mode.

Fig. 6(a) shows the three-phase current of the primary, which is distorted and unbalanced. The existence of the NS component in the primary current under UGVC leads to deviation of the primary current from balanced waveforms. Also, the secondary current, which is shown in Fig. 6(b), contains harmonics as expected according to Eq. (5). Absolute value of the fundamental frequency of the secondary current varies proportional with the speed deviation from the synchronous speed. At t = 3 s (synchronous mode), the sign of the frequency is changed from negative values (sub-synchronous mode) to positive values (supper-synchronous mode). Furthermore, Fig. 6(c) shows the electrical torque with a large pulsation. Also, the negative sign of electrical torque indicates generation mode.

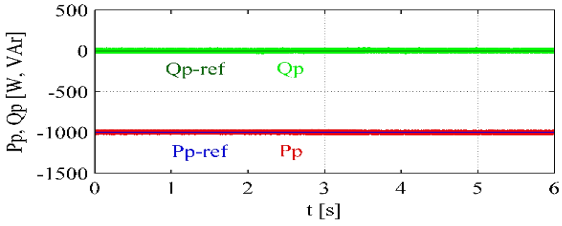

Fig. 5. The primary powers controlled by the original PDPC method

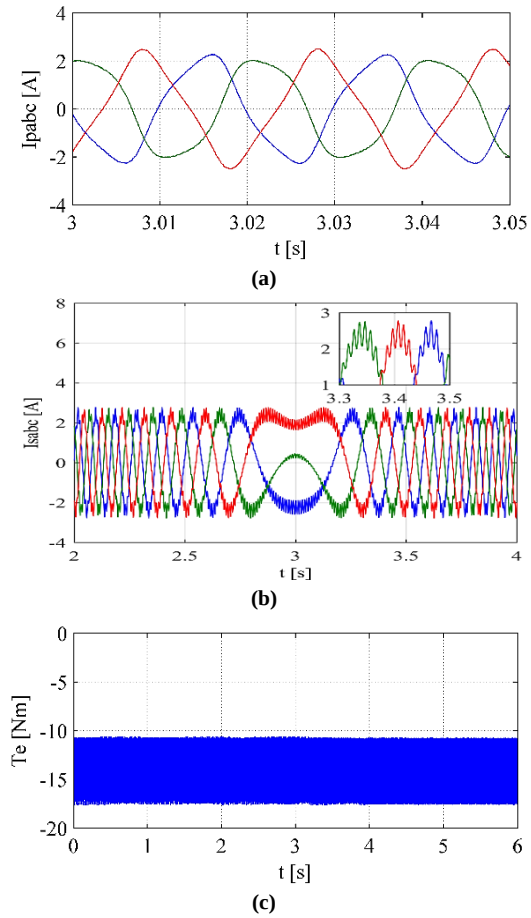

Fig. 6. The results with the original PDPC method: (a) The primary current, (b) the secondary current, (c) the electrical torque

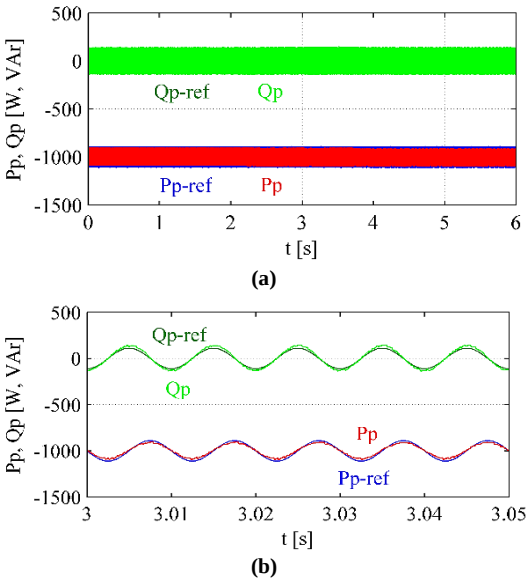

Fig. 7. (a) The primary powers controlled by strategy I of the proposed PDPC method, (b) their extended view

6.2. Control of the BDFRG under UGVC using strategy I

In this subsection, performance of the strategy I of the proposed PDPC method for control of the BDFRG under UGVC has been studied. The control objective of

the strategy I is elimination of the NS component of the primary current to achieve balanced and sinusoidal current. The original active power and reactive power references of the primary are -1000 W and 0 VAr, respectively. $P^*_{p\_comp}$ and $Q^*_{p\_comp}$ obtained from Eqns. (45) and (46) are respectively added to the original active power and reactive power references. Fig. 7 shows the oscillating power references, which adequately followed by the active power and reactive power during the speed variation.

Fig. 8(a) shows that the three-phase current of the primary is almost balanced and sinusoidal, because of elimination of NS component of the primary current. By using the strategy I, the waveforms of the primary current are improved in comparison to the results of the original PDPC method (Fig. 6(a)). In Fig. 8(b), the three-phase current of the secondary has been illustrated. It can be seen that the amplitude of harmonics in the secondary current is smaller than Fig. 6(b) (original PDPC method). In Fig. 8(c), the electrical torque has smaller pulsation in comparison to the original PDPC method (Fig. 6(c)), due to elimination of NS component of the primary current. Although, the control objective of the strategy I is just balancing of the primary current.

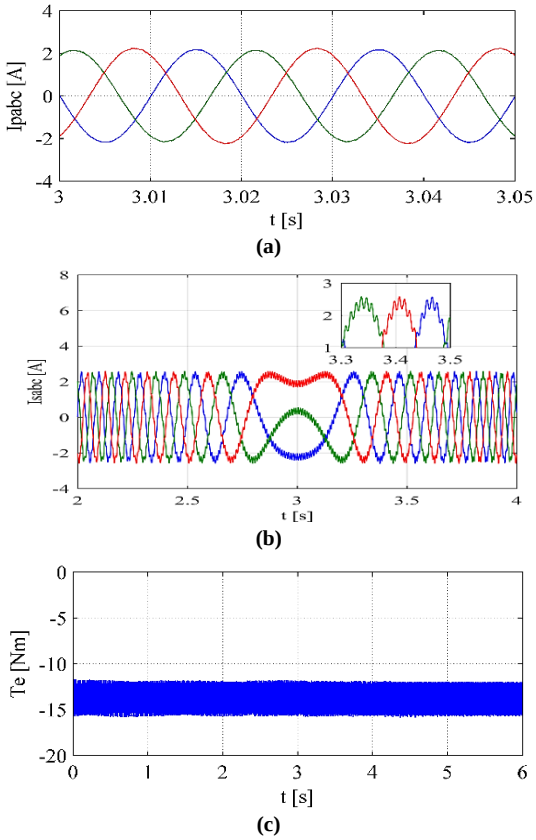

Fig. 8. The results with strategy I of the proposed PDPC method: (a) the primary current, (b) the secondary current, (c) the electrical torque

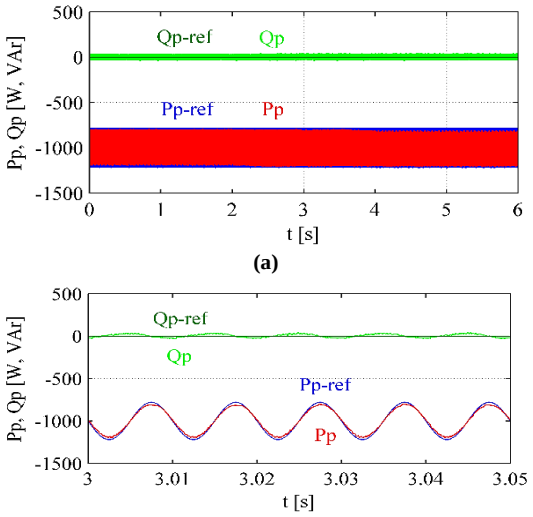

Fig. 9. (a) The primary powers controlled by strategy II of the proposed PDPC method, (b) their extended view

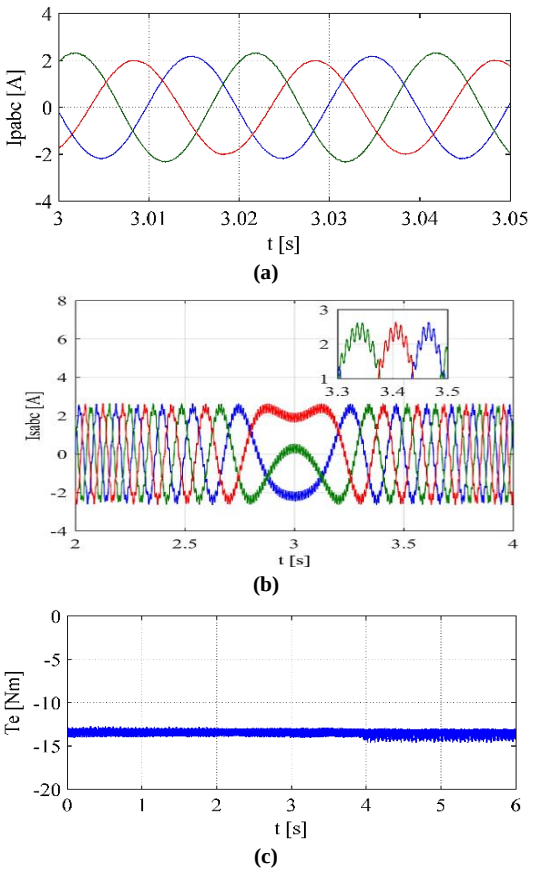

Fig. 10. The results with strategy II of the proposed PDPC method: (a) the primary current, (b) the secondary current, (c) the electrical torque

6.3. Control of the BDFRG under UGVC using strategy II

In this subsection, the operation of the BDFRG using strategy II of the proposed PDPC method has been studied. The control objective is elimination of the electrical torque pulsation under UGVC. Therefore, $P^*_{p\_comp}$ obtained from (57) is added to the original

active power reference. According to (58), the compensating reactive power reference ($Q^*_{p\_comp}$) is zero. So, the new reactive power reference is the same as the original reactive power reference. Similar to the previous subsections, the original active power and reactive power references are -1000 W and 0 VAr, respectively. The primary powers, which are controlled by the strategy II of the proposed PDPC method, adequately track their references in Fig. 9.

Fig. 10(a) shows the three-phase unbalanced current of the primary, which is improved respect to the original PDPC method (Fig. 6(a)), and has sinusoidal waveforms. In Fig. 10(b), the three-phase current of the secondary contains less harmonics than the current illustrated in Fig. 6(b) (the original PDPC method). However, the primary and secondary currents of the strategy I (Fig. 8(a) and Fig. 8(b)) have the best responses. In Fig. 10(c), the electrical torque pulsation is greatly decreased respect to pulsation of two previous methods (Fig. 6(c) and Fig. 8(c)).

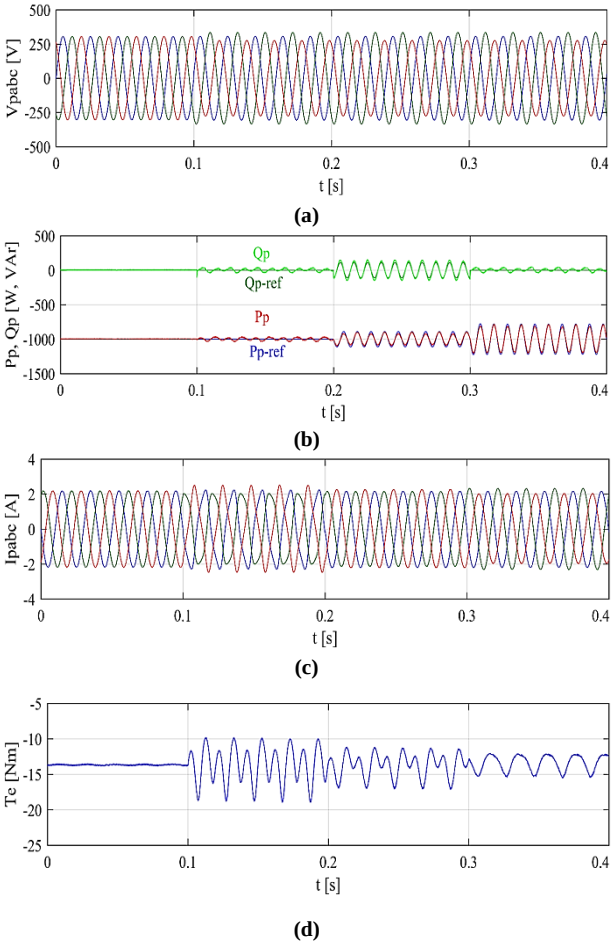

Fig. 11. The BDFRG results for the presented control methods: (a) the primary voltage, (b) the primary active and reactive powers and their reference values, (c) the primary current, (d) the electrical torqu

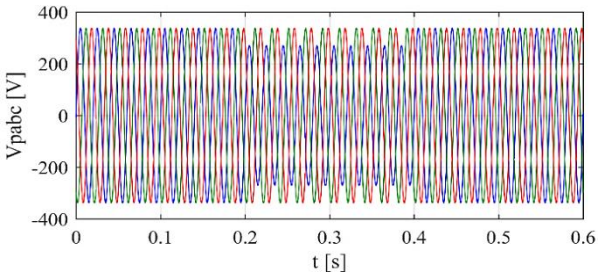

Fig. 12. The primary voltage with single-phase voltage dip

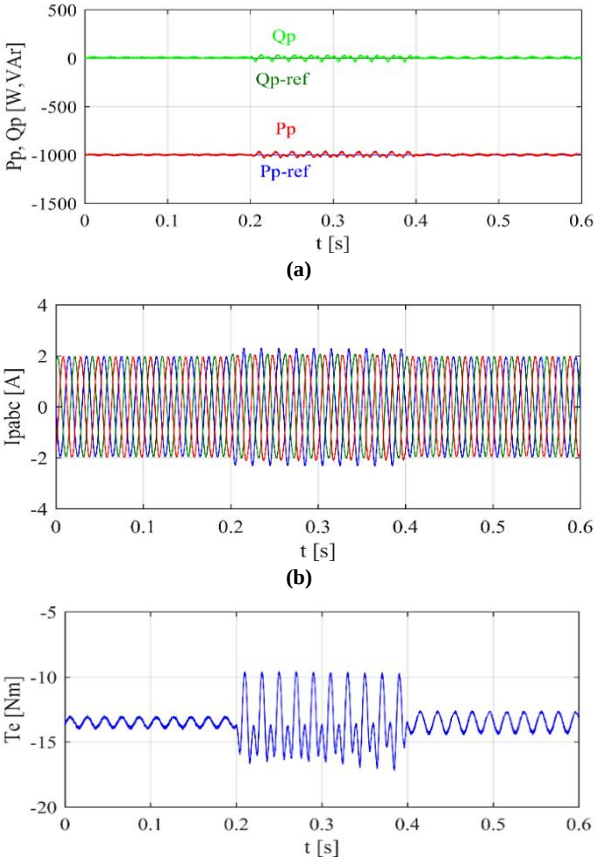

Fig. 13. The BDFRG results with the original PDPC method under single-phase voltage dip: (a) the primary active and reactive powers and their reference values, (b) the primary current, (c) the electrical torque

6.4. Comparison of the control methods

In this subsection, another test has been designed for better comparison of the presented control methods in the previous subsections. The test is performed for evaluation of dynamic response characteristics in moving from balanced condition to UGVC and between the control methods. For this test, the BDFRG speed is controlled to 800 rpm. The grid voltage, which is applied to the BDFRG primary (Fig. 11(a)), is balanced between t = 0 s to t = 0.1 s and is unbalanced between t = 0.1 s to t = 0.4 s (with unbalanced factor of 11.11%). Between t = 0 s to t = 0.1 s, the BDFRG is controlled with the original PDPC method under balanced condition. At t = 0.1 s, the grid voltage is changed to an

unbalanced voltage. Between t = 0.1 s to t = 0.2 s, the BDFRG is still controlled by the original PDPC method under UGVC (without applying a compensation strategy). At t = 0.2, the control method is changed to strategy I of the proposed PDPC method, and the BDFRG is controlled by this method under UGVC up to t = 0.3 s. At t = 0.3, the control method is changed to strategy II of the proposed PDPC method, and the BDFRG is controlled by this method under UGVC up to t = 0.4 s. The test results for the BDFRG primary powers, primary current, and electrical torque have been shown in Fig. 11(b), Fig. 11(c), and Fig. 11(d), respectively. The good power tracking can be observed for all four time intervals as well as in condition transition. Also, it can be observed that the best result for the primary current and electrical torque is related to the proposed strategy I and strategy II, respectively. Furthermore, quantified comparison of the control methods is presented in Table 1.

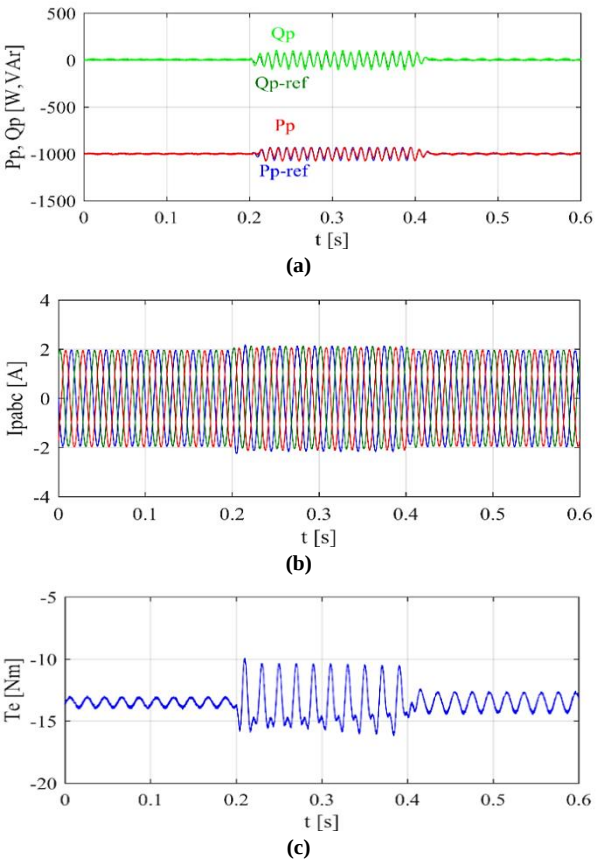

Fig. 14. The BDFRG results with strategy I of the proposed PDPC method under single-phase voltage dip: (a) the primary active and reactive powers and their reference values, (b) the primary current, (c) the electrical torque

6.5. Performance of the control methods under unbalanced voltage dips

In this subsection, the operation of the BDFRG under unbalanced voltage dips with the original PDPC method and proposed PDPC method (strategies I & II) has been studied. A single-phase voltage dip is considered in the grid by dropping the voltage to 80% of its normal value for 200 ms interval, according to Ref. [41]. It should be noted that, when the primary of the BDFRG is connected with a star-star-connected transformer to the grid (or it is directly connected to the grid), the primary experiences a similar single-phase voltage dip. However, when the primary is connected through a star-delta-connected transformer to the grid, the voltage of the primary experiences a two-phase voltage dip [41]. The following tests have been performed under both of the mentioned conditions with the original PDPC method and proposed PDPC method (strategies I & II). Also, the BDFRG speed is controlled to be 800 rpm during the tests.

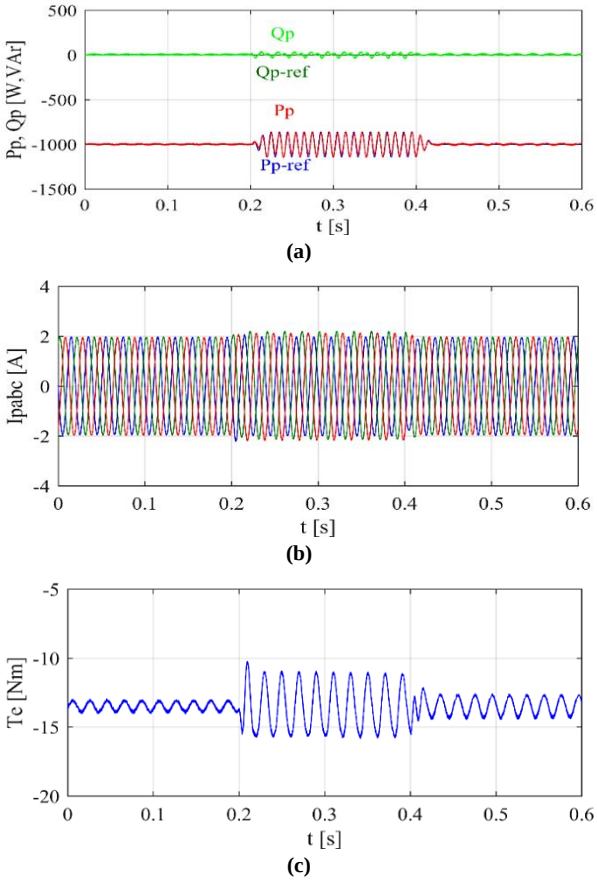

Fig. 15. The BDFRG results with strategy II of the proposed PDPC method under single-phase voltage dip: (a) the primary active and reactive powers and their reference values, (b) the primary current, (c) the electrical torque

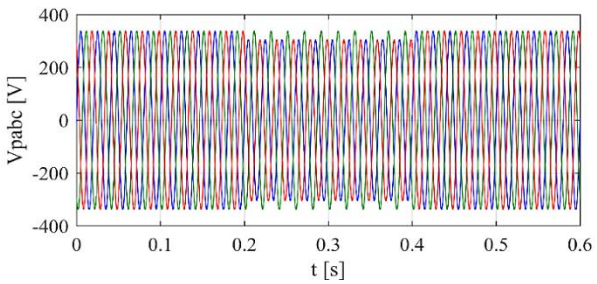

Fig. 16. The primary voltage with two-phase voltage dip

Table 1. Quantified comparison of the BDFRG results for the presented control methods

Conditions	Balanced condition	UGVC		
Control Methods / Parameters	The original PDPC	The original PDPC	The proposed PDPC (Strategy I)	The proposed PDPC (Strategy II)
Unbalance factor of the primary current (%)	-	11.5	2.5	8.5
The electrical torque ripple (Nm)	0.4	9.3	6.1	3.5
THD of the secondary current (%)	0.5	13	10.5	11.8

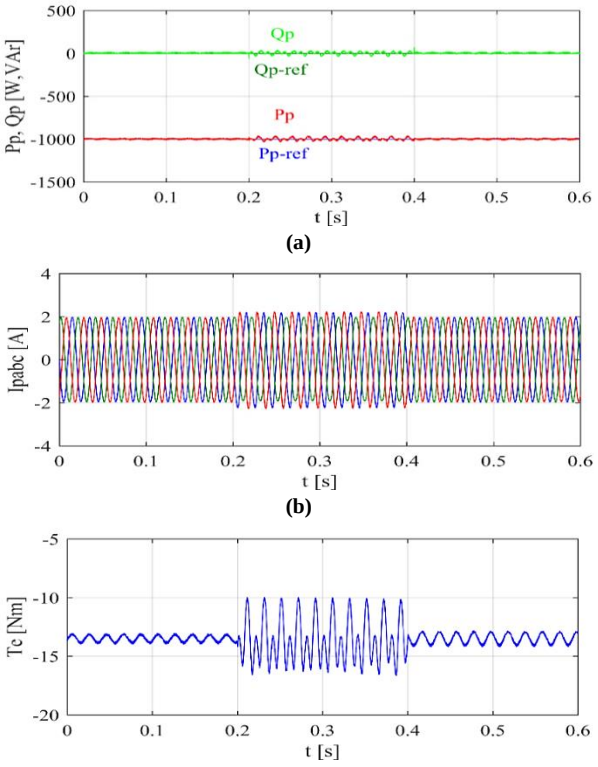

Fig. 17. The BDFRG results with the original PDPC method under two-phase voltage dip: (a) the primary active and reactive powers and their reference values, (b) the primary current, (c) the electrical torque

Fig. 12 shows the primary voltage with a single-phase dip. The related BDFRG results with the original PDPC method, strategy I of the proposed PDPC method, and strategy II of the proposed PDPC method have been illustrated in Fig. 13, Fig. 14, and Fig. 15, respectively. It can be observed that the primary active and reactive powers track their reference values using all three methods. The best result for the primary current is dedicated to the strategy I of the proposed PDPC method, where the primary has almost balanced current during the unbalanced voltage dip. Also, the minimum electrical torque pulsation is related to the strategy II of the proposed PDPC method.

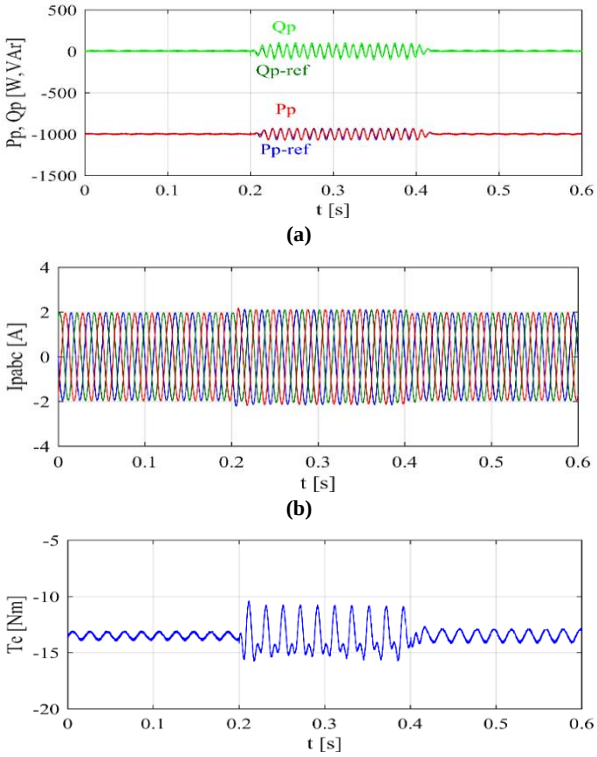

Fig. 18. The BDFRG results with strategy I of the proposed PDPC method under two-phase voltage dip: (a) the primary active and reactive powers and their reference values, (b) the primary current, (c) the electrical torque

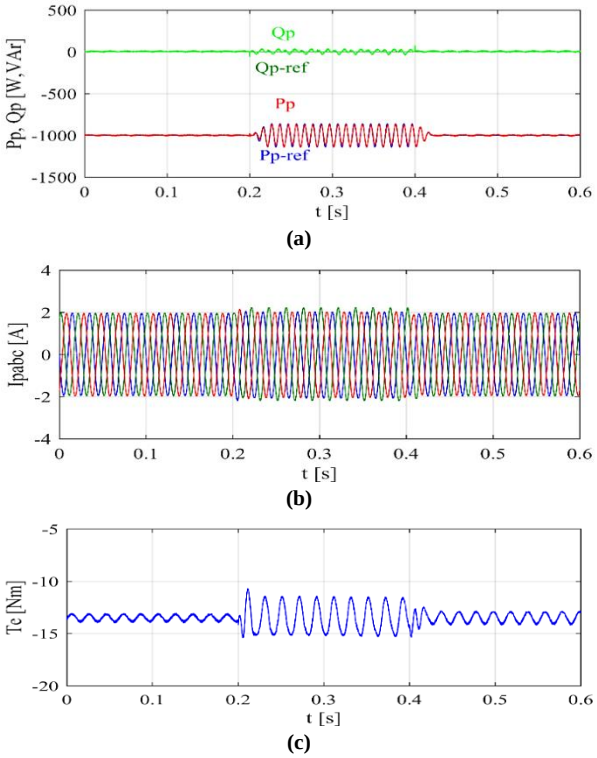

Fig. 19. The BDFRG results with strategy II of the proposed PDPC method under two-phase voltage dip: (a) the primary active and reactive powers and their reference values, (b) the primary current, (c) the electrical torque

In the next tests, a two-phase voltage dip occurs in the primary voltage (Fig. 16). The BDFRG results with the original PDPC method, strategy I of the proposed PDPC method, and strategy II of the proposed PDPC method are shown in Fig. 17, Fig. 18, and Fig. 19, respectively. Similar to previous tests, all three methods have a good performance in power tracking. Also, The primary current by the strategy I is almost balanced, and the minimum electrical torque pulsation is related to the strategy II.

7. CONCLUSIONS

In the present paper, operation of the BDFRG under UGVC has been studied. A PDPC method, based on power compensation strategy, has been proposed by defining two different strategies with the following control objectives: (1) to reach balanced current of the primary, and (2) to remove the electrical torque pulsation. To achieve the control objectives, new appropriate power references have been defined by using the PS and NS equations of the BDFRG. Simulink toolbox of MATLAB software has been used to simulate the system model, and investigation of the BDFRG operation under UGVC. By applying the original PDPC method (without using any compensation strategy), the primary current is distorted and unbalanced, and the electrical torque has large pulsation. By using the strategy I of the proposed PDPC method, the primary current is sinusoidal and balanced. In addition, the pulsation of the electrical torque is reduced. By using the strategy II of the proposed PDPC method, the pulsation of the electrical torque is significantly removed. The primary current is sinusoidal, although it is still unbalanced. So, the proposed control strategies can successfully control the BDFRG under UGVC according to their control objectives. Future works can be dedicated to design of other control methods for the BDFRG under UGVC such as vector methods, or control of the BDFRG under UGVC by controlling the grid side converter.

Acknowledgement

The authors wish to thank Sahand University of Technology.

REFERENCES

[1] A. B. Attya, S. Ademi, M. Jovanović and O. Anaya-Lara, “Frequency support using doubly fed induction and reluctance wind turbine generators”, *Int. J. Electr. Power Energy Syst.*, vol. 101, pp. 403-14, 2018.

[2] M. Jovanović and S. Ademi, “Simulation and practical studies of doubly-fed reluctance drives operation and control”, in Proc. of the *11th Int. Symp. Diagn. Electr. Mach., Power Electron. Drives*,pp. 346-52, 2017.

[3] V.T. Phan, T. Logenthiran, W. L. Woo, D. Atkinson and V. Pickert, “Analysis and compensation of voltage unbalance of a DFIG using predictive rotor current control”, *Int. J. Electr. Power Energy Syst.*, vol. 75, pp. 8-18, 2016.

[4] M. Darabian, A. Jalilvand and R. Noroozian, “Combined use of sensitivity analysis and hybrid Wavelet-PSO-ANFIS to improve dynamic performance of DFIG-based wind generation”, *J. Oper. Autom. Power Eng.*, vol. 2, no. 1, pp. 60-73, 2014.

[5] J. Poza, E. Oyarbide, D. Roye and M. Rodriguez, “Unified reference frame dq model of the brushless doubly fed machine”, *IET Electr. Power App.*, vol. 153, no. 5, pp. 726-734, 2006.

[6] R. E. Betz and M. G. Jovanovic, “Theoretical analysis of control properties for the brushless doubly fed reluctance machine”, *IEEE Trans. Energy Convers.*, vol. 17, no. 3, pp. 332-329, 2002.

[7] M. G. Jovanovic, R. E. Betz and Y. Jian, “The use of doubly fed reluctance machines for large pumps and wind turbines”, *IEEE Trans. Ind. Appl.*, vol. 38, no. 6, pp. 1508-1516, 2002.

[8] H. Chaal and M. Jovanovic, “Power control of brushless doubly-fed reluctance drive and generator systems”, *Renew. Energy*, vol. 37, no. 1, pp. 419-425, 2012.

[9] R. S. Rebeiro and A. M. Knight, “Two-converters-based synchronous operation and control of a brushless doubly fed reluctance machine”, *IEEE Trans. Magn.*, vol. 54, no. 11, pp. 1-5, 2018.

[10] W. Fengxiang, Z. Fengge and X. Longya, “Parameter and performance comparison of doubly fed brushless machine with cage and reluctance rotors”, *IEEE Trans. Ind. Appl.*, vol. 38, no. 5, pp. 1237-1243, 2002.

[11] M. Moazen, R. Kazemzadeh and M. R. Azizian, “Power control of BDFRG variable-speed wind turbine system covering all wind velocity ranges”, *Int. J. Renew. Energy Res.*, vol. 6, no. 2, pp. 477-486, 2016.

[12] M. G. Jovanovic, R. E. Betz, Y. Jian and E. Levi, “Aspects of vector and scalar control of brushless doubly fed reluctance machines”, in Proc. *4th IEEE Int. Conf. Power Electron. Drive Syst.*,pp. 461-467, 2001.

[13] M. Hassan and M. Jovanovic, “Improved scalar control using flexible DC-Link voltage in brushless doubly-fed reluctance machines for wind applications”, in Proc. *2nd Int. Symp. Environ. Friendly Energies Appl.*,pp. 482-487, 2012.

[14] M. G. Mousa, S. Allam and E. M. Rashad, “Sensored and sensorless scalar-control strategy of a wind-driven BDFRG for maximum wind-power extraction”, *J. Control Decis.*, pp. 1-19, 2017.

[15] M. Jovanovic, “Sensored and sensorless speed control methods for brushless doubly fed reluctance motors”, *IET Electr. Power Appl.*, vol. 3, pp. 503-513, 2009.

[16] S. Ademi and M. Jovanovic, “Vector control strategies for brushless doubly-fed reluctance wind generators”, in Proc. *2nd Int. Symp.Environment Friendly Energies*

Appl, Newcastle upon Tyne, pp. 44-49,2012.

[17] S. Ademi, M. G. Jovanovic and M. Hasan, "Control of brushless doubly-fed reluctance generators for wind energy conversion systems", *IEEE Trans. Energy Convers.*, vol. 30, no. 2, pp. 596-604, 2015.

[18] M. G. Mousa, S. Allam and E. M. Rashad, "Maximum power extraction under different vector-control schemes and grid-synchronization strategy of a wind-driven brushless doubly-fed reluctance generator", *ISA Trans.*, vol. 72, pp. 287-97, 2018.

[19] X. Longya, L. Zhen and K. Eel-Hwan, "Field-orientation control of a doubly excited brushless reluctance machine", *IEEE Trans. Ind. Appl.*, vol. 34, no. 1, pp. 148-155, 1998.

[20] S. Ademi, M. G. Jovanovic, H. Chaal and W. Cao, "A new sensorless speed control scheme for doubly fed reluctance generators", *IEEE Trans. Energy Convers.*, vol. 31, no. 3, pp. 993-1001, 2016.

[21] M. Jovanovic, J. Yu and E. Levi, "Direct torque control of brushless doubly fed reluctance machines", *Electr. Power Compon. Syst.*, vol. 32, pp. 941-958, 2004.

[22] H. Chaal and M. Jovanovic, "Practical implementation of sensorless torque and reactive power control of doubly fed machines", *IEEE Trans. Ind. Electron.*, vol. 59, no. 6, pp. 2645-2653, 2012.

[23] M. Jovanović and H. Chaal, "Wind power applications of doubly-fed reluctance generators with parameter-free hysteresis control", *Energy Convers. Manage.*, vol. 134, pp. 399-409, 2017.

[24] M. Moazen, R. Kazemzadeh and M. R. Azizian, "Model-based predictive direct power control of brushless doubly fed reluctance generator for wind power applications", *Alexandria Eng. J.*, vol. 55, no. 3, pp. 2497-2507, 2016.

[25] D. Gay, R. E. Betz, D. Dorrell and A. Knight, "Brushless doubly fed reluctance machine testing for parameter determination", *IEEE Trans. Ind. Appl.*, vol. 55, no. 3, pp. 2611-2619, 2019.

[26] K. Kiran and S. Das, "Implementation of reactive power-based MRAS for sensorless speed control of brushless doubly fed reluctance motor drive", *IET Power Electron.*, vol. 11, no. 1, pp. 192-201, 2018.

[27] M. Kumar and S. Das, "Model reference adaptive system based sensorless speed estimation of brushless doubly-fed reluctance generator for wind power application", *IET Power Electron.*, vol. 11, no. 14, pp. 2355-2366, 2018.

[28] M. Kumar, S. Das and K. Kiran, "Sensorless speed estimation of brushless doubly-fed reluctance generator using active power based MRAS", *IEEE Trans. Power Electron.*, vol. 34, pp. 7878-7886, 2018.

[29] T. K. A. Brekken and N. Mohan, "Control of a doubly fed induction wind generator under unbalanced grid voltage conditions", *IEEE Trans. Energy Convers.*, vol. 22, no. 1, pp. 129-135, 2007.

[30] R. Cardenas, R. Pena, S. Alepuz and G. Asher, "Overview of control systems for the operation of DFIGs in wind energy applications", *IEEE Trans. Ind. Electron.*, vol. 60, no. 7, pp. 2776-2798, 2013.

[31] M. Moazen, R. Kazemzadeh and M. R. Azizian, "Mathematical modeling and analysis of brushless doubly fed reluctance generator under unbalanced grid voltage condition", *Int. J. Electr. Power Energy Syst.*, vol. 83, pp. 547-559, 2016.

[32] Y. Wang, L. Xu and B. W. Williams, "Compensation of network voltage unbalance using doubly fed induction generator-based wind farms", *IET Renew. Power Gener.*, vol. 3, no. 1, pp. 12-22, 2009.

[33] A. Nafar, G. R. Arab Markadeh and A. Elahi, "Low voltage ride through enhancement based on improved direct power control of dfig under unbalanced and harmonically distorted grid voltage", *J. Oper. Autom. Power Eng.*, vol. 4, no. 1, pp. 16-28, 2016.

[34] H. Jiefeng, Z. Jianguo and D. G. Dorrell, "Model-predictive direct power control of doubly-fed induction generators under unbalanced grid voltage conditions in wind energy applications", *IET Renew. Power Gener.*, vol. 8, no. 6, pp. 687-695, 2014.

[35] J. Hu, J. Zhu and D. G. Dorrell, "Predictive direct power control of doubly fed induction generators under unbalanced grid voltage conditions for power quality improvement", *IEEE Trans. Sustain. Energy*, vol. 6, no. 3, pp. 943-950, 2015.

[36] R. E. Betz and M. G. Jovanovic, "Introduction to the space vector modeling of the brushless doubly fed reluctance machine", *Electr. Power Compon. Syst.*, vol. 31, no. 8, pp. 729-755, 2003.

[37] R. Betz and M. Jovanovic. "Introduction to brushless doubly fed reluctance machines-the basic equations", *Tech. Rep., Dept. Elec. Energy Conversion, Aalborg Univ., Denmark*, 1998.

[38] A. Iqbal, A. Lamine and I. Ashraf, "Matlab/simulink model of space vector PWM for three-phase voltage source inverter", in Proc. *41st Int. Universities Power Eng. Conf.*, Newcastle-upon-Tyne, pp. 1096-1100,2006.

[39] M. G. Jovanovic, Y. Jian and E. Levi, "Encoderless direct torque controller for limited speed range applications of brushless doubly fed reluctance motors", *IEEE Trans. Ind. Appl.*, vol. 42, no. 3, pp. 712-22, 2006.

[40] A. Bouafia, J. P. Gaubert and F. Krim, "Predictive direct power control of three-phase pulsewidth modulation (PWM) rectifier using space-vector modulation (SVM)", *IEEE Trans. Power Electron.*, vol. 25, no. 1, pp. 228-236, 2010.

[41] H. Nian, Y. Song, P. Zhou and Y. He, "Improved direct power control of a wind turbine driven doubly fed induction generator during transient grid voltage unbalance", *IEEE Trans. Energy Convers.*, vol. 26, no. 3, pp. 976-86, 2011.